

# CFD simulation of gas–solid bubbling fluidized bed: an extensive assessment of drag models

N. Mahinpey<sup>1</sup>, F. Vejahati<sup>1</sup> & N. Ellis<sup>2</sup>

<sup>1</sup>*Environmental Systems Engineering, Faculty of Engineering,  
University of Regina, Regina, Saskatchewan, Canada*

<sup>2</sup>*Department of Chemical and Biological Engineering,  
University of British Columbia, Vancouver, BC, Canada*

## Abstract

In the computational fluid dynamics modeling of gas–solid two phase flow, drag force is one of the dominant mechanisms for interphase momentum transfer. Despite the profusion of drag models, an extensive comparison is missing from the literature. In this work the drag correlations of Syamlal-O'Brien, Gidaspow, Wen-Yu, Arastoopour, Gibilaro, Di Felice, Zhang-Reese and Koch *et al.* are reviewed using a multifluid model of FLUENT software with the resulting hydrodynamics parameters being compared with experimental data. Also adjustment of drag models based on minimum fluidization was studied. A new method adopted to adjust the drag function of Di Felice showed a quantitative improvement compared to the adjusted drag model of Syamlal-O'Brien. Prediction of bed expansion and pressure drop showed excellent agreement with results of experiments conducted in a Plexiglas fluidized bed. A mesh size sensitivity analysis with varied interval spacing showed that mesh interval spacing with 18 times the particle diameter and using higher order discretization methods produces acceptable results.

*Keywords:* multiphase flow, fluidization, computation, modeling, CFD, drag models, two-dimensional.

## 1 Introduction

Studies conducted on the dynamics of a single particle in a fluid have proven several mechanisms of momentum transfer between phases: drag force, caused by velocity differences between the phases; buoyancy, caused by the fluid



pressure gradient; virtual mass effect, caused by relative acceleration between phases; Saffman lift force, caused by fluid-velocity gradients; Magnus force, caused by particle spin; Basset force, which depends upon the history of the particle's motion through the fluid; Faxen force, which is a correction applied to the virtual mass effect; Basset force to account for fluid-velocity gradients; and forces caused by temperature and density gradients [1]. Several factors should be considered in extension of single particle model to describe interaction forces in multi-particle systems, including the effect of the proximity of other particles, which implies that the drag force is a function of solid volume fraction, in addition to the particle Reynolds number. Also the single-particle interaction force must be corrected to account for the effect of mass transfer between the phases, and the momentum transfer accompanying such mass transfer must be included in the interaction force. Buoyancy, drag, and momentum transfer due to mass transfer have been considered as controlling mechanisms of gas–solid momentum transfer, since they are the dominant forces as a result of the large density difference between the particles and the fluidizing gas and also due to lack of satisfactory formulations of the other forces. Whilst the inherent instabilities due to inclusion of buoyancy are still not resolved, prediction of a drag model that covers the whole range of Reynolds number and phasic volume fraction has been looked at as the main challenge of numerous of the studies in multiphase flow modeling [2]. These attempts have resulted in the appearance of a substantial number of drag correlations in the literature.

The copiousness of drag models available in the literature and the selective attitudes of some researchers have resulted in some inconsistencies regarding the appropriate comparison of available drag models. Almost all the available studies have included efforts to compare two, or at most three, drag correlations, and occasionally the discrepancies between the reported results in modeling fluidization hydrodynamics are easily observed. In this respect, the underlying objective of this study is to accomplish an extensive assessment of frequently used drag correlations in a large selection of published literature and provide a comprehensive comparison between simulation and experimental results using the variety of the drag models. Also, a new approach to adjust the drag model, based on minimum fluidization velocity, is proposed and compared with experimental values. CFD simulation was carried out using the commercial CFD code, FLUENT.

## 2 Model equations

The drag force depends on the local relative velocity between phases and void fraction and some other factors, such as particle size distribution, particle shape, *etc.* However, void fraction dependency is very difficult to be determined for any conditions other than a packed bed or infinite dilution (single particle). Also, some factors, like particle size distribution, particle shape, and particle clustering have not been considered in deriving drag correlations. In an ideal case, it could only be determined how the drag for specific material varies with local “slip” velocity and packing, although, totally unrealistic. On the other hand, most

researchers have information on the minimum fluidization velocity of their own material. In this respect, Syamlal and O'Brien [3] introduced a method to adjust drag law using minimum fluidization velocity as a calibration point. This adjustment has been introduced in order to make the drag law more accurate for a specific system under study. However, this method requires measurement of the minimum fluidization velocity and void fraction of the bed at minimum fluidization velocity by means of experimentation.

As another alternative based on the same concept used by Syamlal and O'Brien [3], we developed the following method to adjust the Di Felice drag model. Di Felice [4] expressed the drag coefficient model as the product of drag force on an unhindered particle subjected to the same volumetric flux of fluid and a voidage function:

$$K_{gs} = \frac{3}{4} C_D \frac{\alpha_s \rho_g}{d_s} |\vec{v}_s - \vec{v}_g| f(\alpha_s) \quad (1)$$

where  $f(\alpha_s)$  is defined as

$$f(\alpha_s) = (1 - \alpha_s)^{-x} \quad (2)$$

and the empirical coefficient ( $x$ ) as a function of  $Re_s$  is expressed as

$$x = P - Q \exp \left[ -\frac{(1.5 - \beta)^2}{2} \right] \quad (3)$$

$$\beta = \log_{10}(Re_s) \quad (4)$$

$$P = 3.7 \quad \& \quad Q = 0.65 \quad (5)$$

In the absence of gas-wall friction and solid stress transmitted by the particles, the momentum balance at minimum fluidization can be written as follows [5]:

$$\begin{aligned} \text{Buoyancy} &= \text{Drag} \\ (1 - \alpha_g) \cdot (\rho_g - \rho_s) g &= \frac{K_{gs}}{\alpha_g} (\vec{v}_g - \vec{v}_s) \end{aligned} \quad (6)$$

At the minimum fluidization velocity, considering that  $\vec{v}_s = 0$  and  $\vec{v}_g = U_{mf}$ , the equation (6) will be reduced to:

$$(1 - \alpha_{g,mf}) \cdot (\rho_g - \rho_s) g = \frac{K_{gs}}{\alpha_{g,mf}} (U_{mf}) \quad (7)$$



Plugging the drag model into Equation (7) and utilizing a nonlinear optimization algorithm the drag model parameters  $P$  &  $Q$  in Equation (3) can be adjusted for the system under study using experimental data at minimum fluidization velocity. However, when adjusting the drag models it should be kept in mind that the adjustment should not alter the behavior of the drag correlation when voidage approaches 1. Most drag correlations are formulated such that in that limit, the single sphere  $C_D$  can be recovered.

### 3 Experimental set-up

The experimental set-up used in this study has been shown in fig. 1. Experiments were carried out in the Department of Chemical and Biological Engineering at the University of British Columbia. The Column is a 2D Plexiglas of 1.2 m height, 0.28 m width, and 0.025 m thickness. Spherical glass beads of 250–300  $\mu\text{m}$  diameter and density 2500  $\text{kg/m}^3$  were fluidized with air at ambient conditions. Pressure drops were measured using three differential pressure transducers located at elevation 0.03, 0.3, and 0.6 m above the gas distributor, respectively. The static bed height of 0.4 m with a solid volume fraction of 0.6 was used in all the experiments. Pressure drop and bed expansion were monitored at different superficial gas velocities ranging from 0 to 0.8 (m/s).

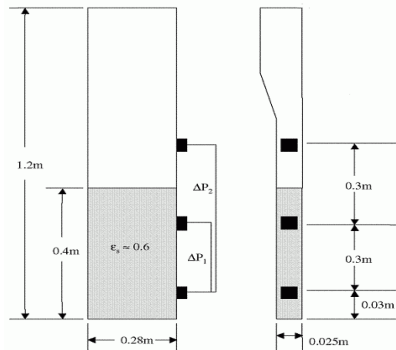


Figure 1: Geometry of 2D Plexiglas fluidized bed.

### 4 Simulation set-up

The two-dimensional (2D) geometry was discretized using 13440 structured rectangular cells. Performing a grid size sensitivity analysis using different mesh sizes, 5 mm mesh interval spacing was chosen for all the simulation runs. The discussion on the effect of the different mesh sizes has been brought up in a later section. A preliminary case study proved that using fixed time step; in order of magnitude  $10^{-3}$ , which has been reported in literature, is not sufficient to avoid the instability in convergence for 2D multiphase simulations. Therefore, an adaptive time-stepping algorithm with 100 iterations per each time step was used

to ensure a stable convergence. The automatic determination of the time step size is based on the estimation of the truncation error associated with the time integration scheme (i.e., first-order implicit or second-order implicit). If the truncation error is smaller than a specified tolerance, the size of the time step is increased; if the truncation error is greater, the time step size is decreased. A minimum value of order  $10^{-5}$  was used for the lower domain of time step. A convergence tolerance of  $10^{-4}$  for each scaled residual component was specified for the relative error between two successive iterations. The governing equations were solved using the finite volume method. The Phase-Coupled SIMPLE algorithm (PC-SIMPLE) [6], which is an extension of the SIMPLE algorithm to multiphase flow, was applied for the pressure-velocity coupling. In this algorithm, the velocities are solved, coupled by phases, in a segregated fashion. Subsequently, the block algebraic multigrid scheme used by the couple solver was used to solve the equation formed by the velocity components of phases at the same time. Also, a pressure correction equation is built based on total volume continuity. Pressure and velocities are then corrected so as to satisfy the continuity constraint. Second-order upwind discretization schemes were used for all the simulation runs. Including the adjusted drag model cases, 9 drag correlations in total, were studied in this work (i.e., Arastoopour, Di Felice, Gibilaro, Gidaspow, Syamlal-O'Brien, Wen-Yu, Zhang-Reese, Koch *et al.*). FLUENT employed an approximate CPU time of 32 hours for 30 s of real-time simulation at a mean time step of 0.0005 s on a double core Sun Microsystems workstation W2100Z with 2 AMD/Opteron 64-bit processors and 4 GB RAM.

## 5 Results and discussion

Experimental runs were conducted to measure the pressure drop and bed expansion ratio,  $H/H_0$ , at different superficial gas velocities. The gas-phase volume fraction from pressure drop measurement across the bed was obtained [7]. At experimentally determined minimum fluidization velocity,  $U_{mf} = 0.065$  m/s, the overall pressure drop, bed expansion ratio, and voidage found to be 4.4 KPa, 1.1, and 0.5, respectively. A wide range of gas superficial velocity (0.011–0.75 m/sec) was considered to measure these parameters. The CFD simulations were carried out using the transient Eulerian-granular model in FLUENT v6.3. Several superficial gas velocities, 0.11, 0.21, 0.38, and 0.46 m/s, which correspond to 1.6, 3.2, 5.8, and  $7U_{mf}$ , respectively studied.

The drag coefficient values as a function of solid volume fraction for different drag models are plotted in Fig. 2. All the drag functions show a rising trend of drag coefficient value with increasing the solid volume fraction. The values of drag coefficients were calculated at a typical Reynolds number,  $Re_s = 10$ . At low volume fraction of solids ( $<0.18$ ), excluding the Syamlal-O'Brien adjusted model, which overestimated and the Arastoopour function, which slightly underestimated the drag coefficient values, all the drag models represent almost the same value of drag function. Also, it should be noted that at the limit of extremely dilute suspension all the drag models approach the single particle drag value. For the values of solid volume fraction above 0.2, the Di Felice adjusted



model precipitously separates from the other model toward the higher values of drag coefficient. This trend continues until it crosses the Syamlal-O'Brien adjusted drag model at the value of solid void fraction equal to 0.46. From this point on, Di Felice adjusted model gives the highest values of the drag coefficient. With the exception of the Syamlal-O'Brien adjusted drag model which shows an decreasing trend regarding the slope of the curve for values of solid volume fraction greater than 0.14, all other models show an approximately constant slope (i.e. linear growth in drag coefficient value). It is also noted that the differences among the drag models mainly occur when the solid volume fraction is higher than 0.2. The graph also reveals that adjustment of drag models based on minimum fluidization velocity results in the prediction of higher values of drag coefficient through the whole range of solid volume fraction.

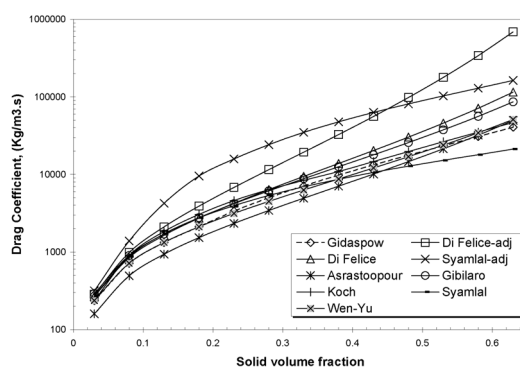


Figure 2: Variation of drag coefficient vs. solid volume fraction in different drag laws.

### 5.1 Bed expansion

Fluctuation and vigorous motion of the bed surface in fluidized beds have made the determination of bed expansion by visual observation a challenging task. The general method employed to determine the bed expansion is normally based on the bed voidage measurement, which in turn is deduced from the mean pressure drop [8]. Also, bed height has been measured experimentally by means of the overhead observation of a probe tip. Such measurement has been believed to be highly biased, and, more importantly, no standard errors or deviations of data have been reported [8]. Fryer and Potter [9] reported that the experimental technique might well underestimate the bed expansion due to the diffusing characteristic of the bed surface. The other frequently employed method is to plot the time-mean gauge pressure (single-point pressure) against the height of the pressure transducer taps, where the intersection of the two slopes corresponds to the height of the expanded bed. However, this method requires an adequate number of pressure transducers at different elevations along the bed and freeboard [10]. In case of a limited number of pressure transducers, Ellis [10], using the time-mean differential pressure drop data across a certain interval

inside the dense bed and across another section extending from the lowest pressure tap to a tap in the freeboard, adopted the following correlation to estimate the expanded bed height:

$$H = \frac{\Delta P_{total}}{\Delta P_{bed}} \Delta Z_{bed} + Z_{bottom\ probe} \quad (8)$$

However, due to the fact that this technique relies on a single pressure drop measurement inside the bed, one should be more cautious about the accuracy of data rather than the method based on the gauge pressure measurement profile.

To determine the bed expansion, from modeling perspective, we considered the height of the bed that contains 95% of the bed weight as the bed height. The results of this method, as reported by Syamlal and O'Brien [8], are not sensitive to the percent bed-weight value chosen within a small range, due to the fact that most of the time, experimental values are reported as bed expansion percent rather than as actual bed height. For this series of simulations, a static bed height of  $H_0=0.4$  m over a range of superficial velocities 11.7, 21, 38, and 46 cm/s was used. All the simulations show the correct qualitative behavior of bed expansion. Ascending trend of bed expansion with increasing superficial gas velocity can be observed from the graph (fig. 3). Also, all the available drag correlations with the exception of two adjusted drag models (i.e. Di Felice and Syamlal-O'Brien) and the original Di Felice drag model at high superficial gas velocity (0.46 m/s), underestimate the bed expansion.

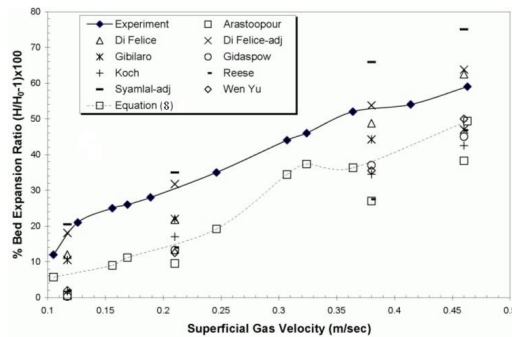


Figure 3: Comparison of simulated bed expansion ratio with experiment data.

## 5.2 Pressure drop

In order to eliminate the large temporal fluctuation of pressure drop in the early seconds of the simulation, the time-average of pressure drop for comparing simulation and experimental results were taken after statistical steady state was established. Numerical results for all the models showed that 3 s of simulation is adequate to reach statistical steady state behavior. Time-averaging was carried out over a range of 4-20 s of real time simulation. As indicated in Fig. 4, the pressure drop inside the bed between two specific elevations (i.e. 0.03 m and 0.3 m as demonstrated in Fig. 1) for all the models showed a declining trend with

increase of the superficial gas velocity, which is in good qualitative agreement with the experimental data. Here again, two adjusted drag models (i.e. Di Felice and Syamlal-O'Brien) showed their superiority in predicting the pressure drop inside the bed. At higher gas velocities,  $7U_{mf}$ , deviation from reported experimental data was observed, which may be explained by the underestimation of the effect of particle clustering at high superficial gas velocities and the influence of the gas distributor at higher velocities.

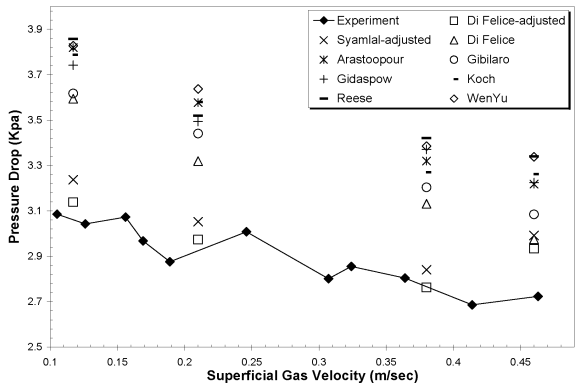


Figure 4: Pressure drop inside the bed  $(\Delta P_1 = \bar{P}_{Z=0.03m} - \bar{P}_{Z=0.3m})$ .

5.3 Grid size sensitivity analysis

To study the effect of mesh size resolution on numerical results, a grid size sensitivity analysis was carried out using three distinctive mesh intervals spacing of 5 mm, 4 mm, and 2 mm for 20 seconds of real-time simulation. The results indicate that the grid size spacing selected for simulation in this work (i.e. 5 mm) was adequate for satisfactory prediction of the hydrodynamics in computational geometry. On the other hand, the results did not support the previously proposed criteria (i.e. adequacy of mesh size less than or equal to 10 times the particle diameter) in the literature, [8,11], for CFD simulation of fluidized beds. Table 1 compares the time required for 20 s of real-time simulation. Required time for simulating 20 seconds of 2D fluidized bed drastically increases from 32 hr to almost one week for a decrease in grid interval spacing from 5 mm to 2 mm, respectively.

Table 1: Grid size sensitivity results.

Mesh spacing (mm)	$\Delta P_1$ (kPa)	$\Delta P_2$ (kPa)	Voidage	Simulation time (hr)
2mm	3.36	5.50	0.55	168
4mm	3.38	5.37	0.54	80
5mm	3.39	5.39	0.54	32





## 6 Conclusion

The influence of most widely used drag functions, including the Wen-Yu, Gidaspow, Di Felice, Syamlal-O'Brien, Zhang-Reese, Arastoopour, Gibilaro, Koch *et al.* models, on CFD simulation of a 2D fluidized bed using FLUENT software was studied. All the models showed an acceptable qualitative agreement with the experimental data. Also, adjustment of drag models based on minimum fluidization velocity showed a quantitative improvement in prediction of hydrodynamics parameters. In this respect, the new method of adjustment based on minimum fluidization velocity in absence of gas-wall friction and solid stress transmission applied on the Di Felice drag model showed excellent agreement with experimental results regarding the prediction of bed expansion and pressure drop inside the bed. The mesh size sensitivity analysis carried out in this study demonstrated that even grid interval spacing of 18 times of the particle size (i.e. 275  $\mu\text{m}$ ) was able to give acceptable results which is contradictory with some other mesh size sensitivity analyses reported in the literature. However, further modeling efforts are required to study the influence of other parameters such as gas distributors, which have not been studied; comparison of 2D and 3D modeling of fluidized bed reactors and also, effect of particle size distribution which has been underestimated using the mean particle diameter. Moreover, new experimental studies should be carried out using recent advancements in instrumentation engineering in order to resolve the available experimental discrepancies reported in the literature such as void fraction measurements, bed expansion ratio *etc.*

## Nomenclature

$C_D$	drag coefficient, dimensionless
$d$	particle mean diameter, m
$f_{drag}$	drag force per unit volume, $\text{N/m}^3$
$\vec{g}$	gravitational acceleration, $\text{m/s}^2$
$H$	expanded bed height, m
$K_{gs}$	gas/solid momentum exchange, $\text{kg/m}^3.\text{s}$
$P$	gas pressure, Pa
$Z$	height coordinate measured from distributor, m

### Greek letters

$\alpha$	gas void fraction
$\rho$	density, $\text{kg/m}^3$
$\vec{v}$	instantaneous velocity vector, m/s



*Subscripts*

g	gas
mf	minimum fluidization
s	solid

**References**

- [1] Johnson, G., Massoudi, M. & Rajagopal, K.R., A review of interaction mechanisms of fluid-solid flows, U.S. DOE, 1990.
- [2] Syamlal, M., Rogers, W. & O'Brien, T. J. MFIx Documentation Theory Guide, 1993.
- [3] Syamlal, M. & O'Brien, T. J. Derivation of a drag coefficient from velocity- voidage correlation; U.S. Department of Energy, Office of Fossil Energy, National Energy Technology Laboratory, Morgantown, WV; April, 1987.
- [4] Di Felice, R., The voidage functions for fluid-particle interaction system. *International Journal of Multiphase Flow*, **20 (1)**, pp. 153–159, 1994.
- [5] Gidaspow, D., Multiphase Flow and Fluidization: Continuum and Kinetic Theory Descriptions. San Diego: Academic Press, 1994.
- [6] Vasquez, S. A., Ivanov, V. A. A phase coupled method for solving multiphase problems on unstructured meshes. In Proceedings of ASME FEDSM'00: ASME 2000 Fluids Engineering Division Summer Meeting; ASME Press: New York, 2000.
- [7] Yang W.C., Handbook of fluidization and fluid-particle systems, New York: Marcel Dekker Inc., 2003.
- [8] Syamlal M., O'Brien T., Fluid dynamic simulation of O<sub>3</sub> decomposition in a bubbling fluidized bed. *AIChE J*, particle tech. and Fluidization, **49(11)**, pp. 2793- 2801, 2003.
- [9] Fryer, C., and O. E. Potter, Experimental investigation of models for fluidized bed catalytic reactors. *AIChE J.*, **22(1)**, pp. 38-47, 1976.
- [10] Ellis N., Hydrodynamics of gas–solid turbulent fluidized beds, PhD thesis, The University of British Columbia, February 2003.
- [11] Zimmermann, S. & Taghipour, F., CFD modeling of the hydrodynamics and reaction kinetics of FCC fluidized bed reactors. *Ind. Eng. Chem. Res.*, **44(26)**, pp. 9818-9827, 2005.

